

## Interference in dielectronic transitions in $\text{H}_2^+ + \text{He}$ collisions

S. F. Zhang,<sup>1,2,\*</sup> X. Ma,<sup>2</sup> and A. B. Voitiv<sup>3,4</sup><sup>1</sup>Max-Planck-Institute for Nuclear Physics, Saupfercheckweg 1, D-69117, Heidelberg, Germany<sup>2</sup>Institute of Modern Physics, Chinese Academy of Sciences, 730000, Lanzhou, China<sup>3</sup>Theoretische Physik I, Heinrich Heine Universität Düsseldorf, Universitätsstraße 1, 40225, Düsseldorf, Germany<sup>4</sup>Institut für Kernphysik, Goethe Universität, Max-von-Laue-Straße 1, D-60438, Frankfurt am Main, Germany

(Received 27 June 2014; published 11 August 2014)

We study single ionization of helium by the impact of the  $\text{H}_2^+$  molecule which in the collision undergoes a transition from the ground state to its first dissociative state. We show that two types of interference effects arise in the spectra of the emitted electrons. One of them is due to the interaction of the atomic electron with the nuclei of the molecule. In the other one the interference is caused by the interaction of this electron with the electron of the molecule. Interference effects of the first type dominate at the low collision velocities due to the effective threshold for the electron-electron interactions.

DOI: [10.1103/PhysRevA.90.022706](https://doi.org/10.1103/PhysRevA.90.022706)

PACS number(s): 34.10.+x, 34.50.Fa, 03.75.-b

### I. INTRODUCTION

Young-type interference in atomic collisions has been extensively studied since the pioneering theoretical work of Tuan and Gerjuoy in 1960 [1]. In their studies, they investigated the electron capture in collisions between protons and  $\text{H}_2$ , and predicted that the capture from two identical centers of  $\text{H}_2$  would lead to interference structures in the cross sections differential in the collision energy.

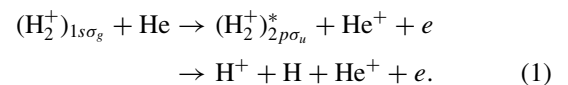
Experimental observation of interference effects in capture collisions was not successful until 1993 when Cheng *et al.* [2] found interference effects in cross sections as a function of the molecular orientation. Later, electron capture were studied for different collision systems involving molecules [3–7].

Interference effects can also arise in electron emission from molecules under ion impact ionization [8,9]. The first results on interference in ionizing collisions were reported in [8] where the single ionization of  $\text{H}_2$  by 60-MeV/u  $\text{Kr}^{34+}$  ions was investigated. There the interference effects were found in the ratio of the measured doubly differential (in emission energy and angle) cross section to the theoretical cross section for ion-impact ionization of atomic hydrogen.

In [10] a strong interference dependence on the electron emission angle was predicted, which was later confirmed experimentally [11–13]. Interference effects were also observed in the cross-section differential in the projectile scattering angle [14,15]. Note that interference effects in the ionization of molecules by the impact of fast bare ions were very recently reviewed in [16].

A qualitatively different situation arises when collisions occur between a molecule and an ion (an atom), which initially has an electron, and interference effects are considered for electron emission from the ion (the atom). In [17] the projectile-electron loss was considered for collisions of highly charged ions with two-atomic molecules. The results of the authors of [17] suggest that pronounced interference effects, which can arise in the electron loss spectra, could be directly observed.

Recently, interference effects were discussed in [18] for the reaction



In that paper, interference effects were discussed for electron emission from the atom by considering the cross-section differential in the transverse momentum transfer in the collision and using the condition that the molecular orientation is perpendicular to the beam direction.

In the present paper we consider the same reaction (1) with electron emission from the atom in a complementary situation where interference effects are studied in the electron emission spectra which are obtained by integrating the fully differential cross section over the transverse momentum transfer. In this situation, in contrast to [18], interference effects are sensitive to the longitudinal momentum transfer, the longitudinal component of the momentum transfer in the collision.

Atomic units are used except where otherwise stated.

### II. GENERAL CONSIDERATION

In the reaction (1) one of the electrons of the atomic target and the electron of the projectile simultaneously undergo transitions. This reaction can be described using perturbation theory in the projectile-target interaction. Let us consider the collision between  $\text{H}_2^+$  and He. Let the nucleus of the target be at rest and taken as the origin. We shall describe the target using the single active electron approximation and denote the initial and final states of this electron by  $\phi_i(\mathbf{r})$  and  $\phi_f(\mathbf{r})$ , respectively, where  $\mathbf{r}$  is the electron coordinate. Further, the initial and final internal states of the  $\text{H}_2^+$  will be approximated by  $[\psi_{1s}(\boldsymbol{\rho} + \boldsymbol{\lambda}/2) \pm \psi_{1s}(\boldsymbol{\rho} - \boldsymbol{\lambda}/2)]/\sqrt{2}$ , where the sign “+” refers to the initial bound state  $1s\sigma_g$ , and the sign “−” to the final dissociated state  $2p\sigma_u$ . Here,  $\psi_{1s}$  is the hydrogen atomic orbital,  $\boldsymbol{\rho}$  is the coordinate of the projectile electron, and  $\boldsymbol{\lambda}$  is the vector connecting the nuclei of the molecule.

\*shaofeng@mpi-hd.mpg.de; zhangshf@impcas.ac.cn

In the first order of perturbation theory, the contribution to the transition amplitude for the reaction (1) is given by

$$A_{fi}^{ee}(\mathbf{q}_\perp) = \frac{2}{q^2 v} \langle \psi_{1s}(\boldsymbol{\rho}) | e^{-i\mathbf{q}\cdot\boldsymbol{\rho}} | \psi_{1s}(\boldsymbol{\rho}) \rangle \sin(\mathbf{q} \cdot \boldsymbol{\lambda}/2) \times \langle \phi_f(\mathbf{r}) | e^{i\mathbf{q}\cdot\mathbf{r}} | \phi_i(\mathbf{r}) \rangle, \quad (2)$$

where  $v$  is the collision velocity and  $\vec{q} = (\vec{q}_\perp, q_\parallel)$  is the momentum transfer in the collision. The longitudinal part of the momentum transfer reads  $q_\parallel = (\Delta E_m + \Delta E_{at})/v$ , where  $\Delta E_m$  and  $\Delta E_{at}$  are the transition energies of the projectile and the target, respectively. Note that according to the first-order perturbation theory only the interaction between the electrons of the target and projectile contributes to the simultaneous transitions of these electrons. Therefore this channel of the reaction (1) can be referred to as the  $ee$  mechanism.

According to the second-order perturbation theory, the main contribution to (1) is given by the reaction channel in which the electron of the target makes a transition due to its interaction with the nuclei of the molecule and the electron of the projectile undergoes the transition due to its interaction with the core of the target (the target nucleus and the passive target electron). The corresponding contribution to the transition amplitude reads

$$A_{fi}^{eN}(\mathbf{q}_\perp) = -i \frac{2Z_{at}}{\pi v^2} \times \int d^2\mathbf{q}_{m,\perp} \frac{1}{q_m^2} \langle \psi_{1s} | e^{i\mathbf{q}_m \cdot \boldsymbol{\rho}} | \psi_{1s} \rangle \sin(\mathbf{q}_m \cdot \boldsymbol{\lambda}/2) \times \frac{1}{q_{at}^2} \langle \phi_f | e^{i\mathbf{q}_{at} \cdot \mathbf{r}} | \phi_i \rangle \cos(\mathbf{q}_{at} \cdot \boldsymbol{\lambda}/2), \quad (3)$$

where  $\mathbf{q}_m = (\mathbf{q}_{m,\perp}, \frac{\Delta E_m}{v})$  is the momentum exchanged between the target core and the projectile electron, and  $\mathbf{q}_{at} = \mathbf{q} - \mathbf{q}_m = (\mathbf{q}_{at,\perp}, \frac{\Delta E_{at}}{v})$  is the momentum transferred between two projectile nuclei and the target electron. In the following, the above second-order channel for the reaction (1) will be referred to as the  $eN$  mechanism.

We note that, compared to the interference of light emitted (scattered) from two slits, the first-order transition amplitude (2) predicts a phase shift of  $\pi$  of the interference fringes in the electron emission spectrum. This phase shift appears because in our case the ‘‘slits’’ themselves undergo a transition. Indeed, according to the first-order perturbation theory, the slits are represented by the electron of  $\text{H}_2^+$ , which itself makes a transition from even  $[\psi_{1s}(\boldsymbol{\rho} + \boldsymbol{\lambda}/2) + \psi_{1s}(\boldsymbol{\rho} - \boldsymbol{\lambda}/2)]/\sqrt{2}$  to odd  $[\psi_{1s}(\boldsymbol{\rho} + \boldsymbol{\lambda}/2) - \psi_{1s}(\boldsymbol{\rho} - \boldsymbol{\lambda}/2)]/\sqrt{2}$  state. This quantum transition introduces the additional phase shift of  $\pi$ .

According to the second-order perturbation theory, the transition of the electron of  $\text{H}_2^+$  is caused by its interaction with the core of the atom whereas the transition of the atomic electron is due to its interaction with the nuclei of the molecule. Since the state of the molecule nuclei (practically) does not change in the collision, here one has a more direct analog to the optical interference and no additional phase shift of  $\pi$  occurs.

From the structure of the first- and second-order transition amplitudes, it is rather obvious that the more pronounced interference in the emission spectrum will take place when the molecular axis is parallel to the collision velocity. Indeed, in such a case the sin and cos terms in the amplitudes (2)

and (3) do not depend on the transverse component of the momentum transfers and, therefore, the integration over these components does not smear out the interference effects. For this parallel orientation of the molecular axis ( $\Theta_M = 0^\circ$ ,  $\Theta_M$  is the angle between the molecular axis and the beam direction) the cross-section differential in the momentum of the emitted electron can be cast into the following form:

$$\frac{d^3\sigma}{dk^3} = \int d^2\mathbf{q}_\perp |A_{fi}^{ee}(\mathbf{q}_\perp) + A_{fi}^{eN}(\mathbf{q}_\perp)|^2 = \sigma_1 \left\{ 1 - \cos \left[ (\Delta E_m + \Delta E_{at}) \frac{\lambda}{v} \right] \right\} + \sigma_2 \left[ 1 + \cos \left( \Delta E_{at} \frac{\lambda}{v} \right) \right] + \sigma_{12} \sin \left[ \left( \frac{\Delta E_m + \Delta E_{at}}{2} \right) \frac{\lambda}{v} \right] \cos \left( \frac{\Delta E_{at} \lambda}{2v} \right), \quad (4)$$

the terms, which are proportional to  $\sigma_1$  and  $\sigma_2$ , correspond to the cross sections obtained by taking into account only the  $ee$  and  $eN$  mechanisms, respectively. The term proportional to  $\sigma_{12}$ , which can be positive or negative, is the result of the interference between these two mechanisms.

The phases of the form  $\Delta E\lambda/v$  in (4), which lead to the interference, can be rewritten as  $\Delta ET$ , where  $T = \lambda/v$  is the time difference between two instances at which the molecular centers pass the target. Thus, the interference in the electron emission spectrum can be thought of as caused by a pair of ‘‘time slits’’ acting on the electron [17].

### III. RESULTS AND DISCUSSION

In Fig. 1 we show the calculated spectra of the electron emitted from the atom neglecting the contribution of the

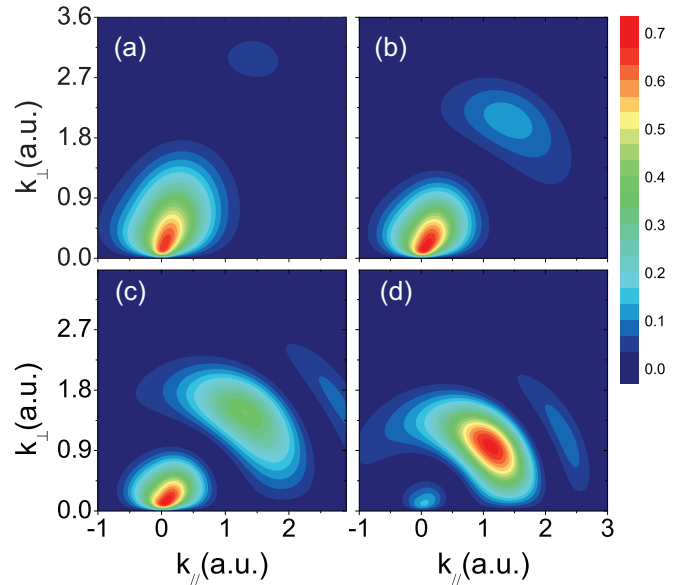


FIG. 1. (Color online) The emission pattern calculated by neglecting the  $ee$  mechanism. (a)–(d) correspond to collision energies of 500, 200, 100, and 50 keV/u, respectively. The molecular polar angle is  $0^\circ$  and  $\lambda = 4$  a.u. In (b), (c), and (d) cross sections  $[\text{Mb}/(\text{a.u.})^2]$  are multiplied by 0.17, 0.07, and 0.02, respectively.

first-order mechanism. This spectrum is given by the cross-section differential in the longitudinal and transverse components of the momentum of the emitted electron and is obtained by integrating the cross section (4) over the azimuthal angle of the emitted electron. The internuclear distance  $\lambda$  was chosen to be 4 a.u. [19]. The spectra are given for different collision energies, which means different values of  $T$ . From Figs. 1(a) to 1(d), the collision energy is 500, 200, 100, and 50 keV/u, corresponding to the time difference of 0.9, 1.4, 2.0, and 2.8 a.u. (0.02, 0.03, 0.05, and 0.07 fs), respectively. Note that these time differences are of the order of the typical transition times in the reaction (1) for the active electron in helium and the electron of the projectile.

If the contribution of the  $ee$  mechanism is ignored, only the second term in the right-hand side of (4) remains and the interference in the calculated spectra arise due to the factor  $1 + \cos(\Delta E_{at}T)$  [see formula (4)]. Therefore, the centers of maxima and minima in the emission spectra are approximately located at  $\varepsilon_k^{(\max)} = \varepsilon_i + 2n\pi/T$  and  $\varepsilon_k^{(\min)} = \varepsilon_i + (2n + 1)\pi/T$ , respectively. Here,  $\varepsilon_i$  and  $\varepsilon_k$  are the initial and final energies of the electron, and  $n$  is a positive integer.

In Fig. 1 we show the emission spectrum as a function of the longitudinal  $k_{\parallel} = \vec{k} \cdot \vec{v}/v$  and transverse  $k_{\perp} = |\vec{k} - (\vec{k} \cdot \vec{v})\vec{v}/v^2|$  parts of the electron momentum  $\vec{k}$ . In accordance with what was discussed in the previous paragraph, it indeed follows from the results shown in Fig. 1 that the spectrum in the coordinates  $(k_{\parallel}, k_{\perp})$  is concentrated on the ridges along the rings corresponding to fixed emission energies. When the collision energy decreases, the time  $T$  increases and the distances between the rings become smaller.

In Fig. 2, we show the emission spectra obtained by taking into account the  $ee$  mechanism and neglecting the  $eN$  mechanism. Note that within such an approximation, only the first term on the right-hand side of (4) remains. Correspondingly, the centers of the maxima and minima in the

emission pattern are given by  $\varepsilon_k^{(\max)} = \varepsilon_i + (2n + 1)\pi/T - \Delta E_m$  and  $\varepsilon_k^{(\min)} = \varepsilon_i + 2n\pi/T - \Delta E_m$ , respectively.

According to the results in Fig. 2, the spectrum shows much less pronounced interference structures. This is related to the effective threshold for the  $ee$  mechanism [20–24]. This mechanism becomes efficient at collision velocities where the energy of an equivelocity free electron satisfies the condition  $v^2/2 \gtrsim k^2/2 + I_b$ , where  $I_b = |\varepsilon_i| + \Delta E_m$ . On the other hand, to observe that there is more than one maximum in the spectrum, the variation of the phase factor  $(\Delta E_m + \Delta E_{at})\lambda/v$  should not be smaller than  $2\pi$ , which means that  $k^2/2$  should vary from 0 to at least  $2\pi v/\lambda$ . Since the collision velocity should not be too low in order that the  $ee$  mechanism is efficient and the emission decreases rather rapidly with increasing  $k$ , one sees that the maxima at higher  $k$  are strongly suppressed.

Figure 3 shows the electron momentum spectra calculated for three different orientations of the molecular axis:  $\Theta_M = 0^\circ, 10^\circ,$  and  $20^\circ$ . The collision energy is 50 keV/u and  $\lambda = 4$  a.u. Taking into account that  $|\varepsilon_i| \approx 0.9$  a.u. and  $\Delta E_m(\lambda = 4 \text{ a.u.}) \approx 0.4$  a.u. [25], we obtain the minimum energy transfer  $I_b \approx 1.3$  a.u. and the corresponding threshold collision velocity  $v_{\text{th}} \approx \sqrt{2I_b} \approx 1.6$  a.u. The later value is above the actual collision velocity ( $v \approx 1.4$  a.u.). Therefore, the  $ee$  mechanism is already suppressed and the spectra mainly feature the interference pattern due to the  $eN$  mechanism.

This can be seen by comparing the left column [Figs. 3(a), 3(c), and 3(e)] and the right column [Figs. 3(b), 3(d), and 3(f)]. The results shown in the left column were obtained by neglecting the  $ee$  mechanism, whereas those in the right column take into account the contributions of both ( $ee$  and  $eN$ ) mechanisms. It is seen that only at small emission energies the  $ee$  mechanism yields substantial contributions, while at higher

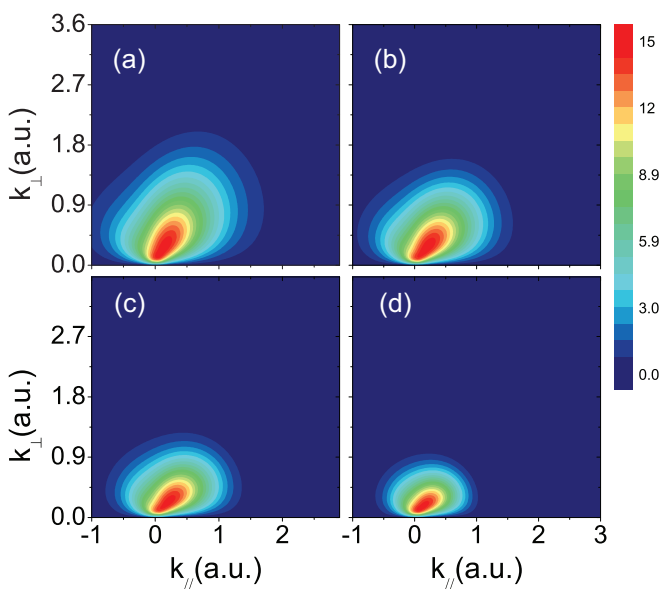


FIG. 2. (Color online) Same as in Fig. 1 but neglecting the  $eN$  mechanism. In (b), (c), and (d) cross sections [Mb/(a.u.)<sup>2</sup>] are multiplied by 0.33, 0.22, and 0.35, respectively.

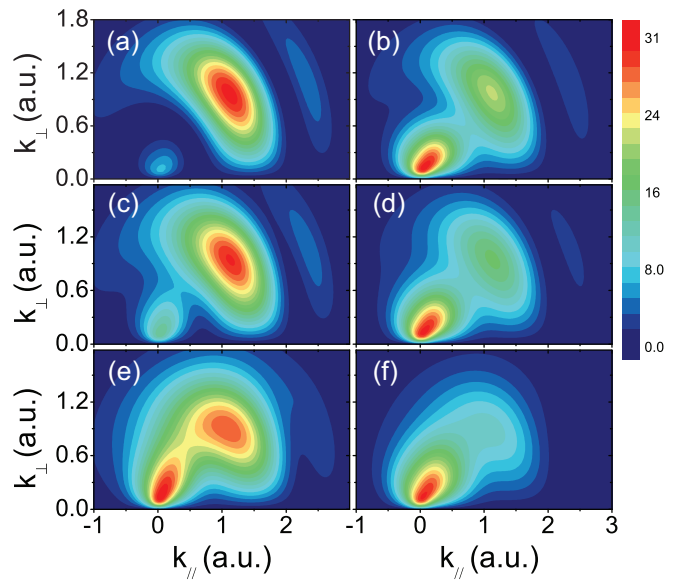


FIG. 3. (Color online) Electron emission spectrum calculated for three different molecular orientations: (a, b)  $\Theta_M = 0^\circ$ , (c, d)  $10^\circ$ , and (e, f)  $20^\circ$ . The collision energy is 50 keV/u, and  $\lambda = 4$  a.u. The results shown in the left column were obtained by neglecting the  $ee$  mechanism. In (b)–(f) cross sections [Mb/(a.u.)<sup>2</sup>] are multiplied by 0.66, 1.19, 0.61, 1.61, and 0.55, respectively.

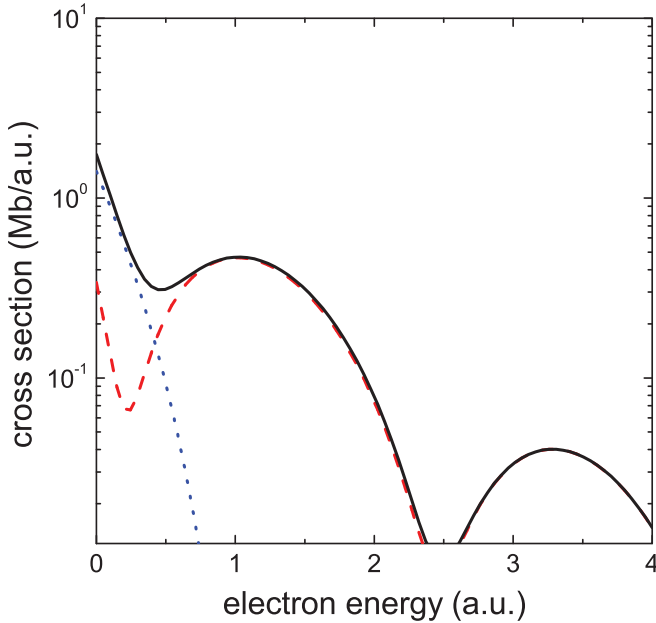


FIG. 4. (Color online) The energy spectrum of the electron emitted in the reaction (1). The orientation angle of the molecules randomly varies between  $0^\circ$  and  $10^\circ$  and  $\lambda = 4$  a.u. The dotted and dashed curves show the contributions of the  $ee$  and  $eN$  mechanisms, respectively. The solid curve is the full result.

energies the emission pattern is practically fully determined by the  $eN$  mechanism alone.

At  $\Theta_M = 0^\circ$  the calculated spectra show a clear interference pattern [see Figs. 3(a) and 3(b)]. However, when the angle  $\Theta_M$  increases the interference rapidly weakens and almost disappears already at  $\Theta_M = 20^\circ$  [see Figs. 3(e) and 3(f)]. The basic reasons for this are two-fold. First, when  $\Theta_M$  increases the effective longitudinal size of the molecule ( $\lambda_{\parallel} = \lambda \cos \Theta_M$ ) decreases, which makes the dependence of the emission pattern on the electron energy oscillating slower. Second, when the molecular axis is not parallel to the collision velocity, the interference pattern depends also on the angle between the transverse momentum transfer and the transverse component of the molecular axis [see formulas (2) and (3)] and the integration over this angle washes out the pattern. This washing out becomes relatively more important when  $\Theta_M$  increases, leading to a gradual decrease in the interference effects.

Interference effects can also be observed in the energy spectrum of the emitted electron. In Fig. 4 we show the energy spectrum for collisions with molecular ions obtained under the assumptions that the orientation angle  $\Theta_M$  of the molecules is

randomly distributed between  $0^\circ$  and  $10^\circ$  and  $\lambda = 4$  a.u. The cross section, averaged over the molecular orientation, was calculated according to

$$\sigma \sim \int_0^{90^\circ} f(\Theta_M) \sigma(\Theta_M) \sin \Theta_M d\Theta_M, \quad (5)$$

where  $\sigma(\Theta_M)$  is the cross section at a given  $\Theta_M$  and

$$f(\Theta_M) = \begin{cases} 1; & 0^\circ \leq \Theta_M \leq 10^\circ, \\ 0; & \Theta_M > 10^\circ. \end{cases}$$

It is seen from the figure that the contribution of the  $ee$  mechanism can be very important at low emission energies, but becomes strongly suppressed at larger energies due to the threshold effect for this mechanism. As a result, the maxima in the spectrum, which are centered at  $Ee \approx 1$  a.u. and  $\approx 3.3$  a.u., arise solely due to the  $eN$  mechanism.

As was already mentioned, the interference effects in the emission spectra rapidly weaken when the angle  $\Theta_M$  increases. We note that according our calculations interference effects in the spectra vanish if the molecules are randomly oriented in space [ $f(\Theta_M) = 1$  for  $0^\circ \leq \Theta_M \leq 90^\circ$ ]. This is because the effects are clearly visible only for small angles  $\Theta_M$  whose contribution to the cross section (5) is suppressed due to the factor  $\sin \Theta_M$ .

#### IV. CONCLUSION

In conclusion, we have studied interference effects in the spectra of electrons emitted in the reaction  $H_2^+ + He \rightarrow H + H^+ + He^+ + e$ . We have shown that the spectra show clear interference effects provided the collision velocity is not too high. The interference appears mainly due to the second-order collision mechanism in which the electron of the target undergoes a transition due to its interaction with the nuclei of the molecular ion, whereas the electron of the ion is excited because of its interaction with the nucleus of the atom. According to our results, the most favorable condition for observing the interference is when the molecular axis is almost parallel to the collision velocity.

The predicted effects can be verified experimentally by colliding a beam of  $H_2^+$  ions with an impact energy of, say, 50 keV/u with a helium target. Using the reaction microscope one can detect in coincidence all the fragments (H,  $H^+$ ,  $He^+$ , and  $e^-$ ) and concentrate only on those events in which the initial internuclear distances in  $H_2^+$  molecules are large enough and the molecules are almost parallel to the beam velocity in order that the interference effects are strong enough. Note that the information about these distances can be obtained from the kinetic energy release and the orientation can be deduced from the momenta of the molecular fragments.

- [1] T. F. Tuan and E. Gerjuoy, *Phys. Rev.* **117**, 756 (1960).  
 [2] S. Cheng, C. L. Cocke, V. Frohne, E. Y. Kamber, J. H. McGuire, and Y. Wang, *Phys. Rev. A* **47**, 3923 (1993).  
 [3] I. Reiser, C. L. Cocke, and H. Bräuning, *Phys. Rev. A* **67**, 062718 (2003).

- [4] H. T. Schmidt, D. Fischer, Z. Berenyi, C. L. Cocke, M. Gudmundsson, N. Haag, H. A. B. Johansson, A. Källberg, S. B. Levin, P. Reinhed, U. Sassenberg, R. Schuch, A. Simonsson, K. Stöckel, and H. Cederquist, *Phys. Rev. Lett.* **101**, 083201 (2008).

- [5] L. P. H. Schmidt, S. Schössler, F. Afaneh, M. Schöffler, K. E. Stiebing, H. Schmidt-Böcking, and R. Dörner, *Phys. Rev. Lett.* **101**, 173202 (2008).
- [6] D. Misra, H. T. Schmidt, M. Gudmundsson, D. Fischer, N. Haag, H. A. B. Johansson, A. Källberg, B. Najjari, P. Reinhed, R. Schuch, M. Schöffler, A. Simonsson, A. B. Voitkiv, and H. Cederquist, *Phys. Rev. Lett.* **102**, 153201 (2009).
- [7] L. P. H. Schmidt, J. Lower, T. Jahnke, S. Schöbller, M. S. Schöffler, A. Menssen, C. Lévéque, N. Sisourat, R. Taïeb, H. Schmidt-Böcking, and R. Dörner, *Phys. Rev. Lett.* **111**, 103201 (2013).
- [8] N. Stolterfoht, B. Sulik, V. Hoffmann, B. Skogvall, J. Y. Chesnel, J. Rangama, F. Frémont, D. Hennecart, A. Cassimi, X. Husson, A. L. Landers, J. A. Tanis, M. E. Galassi, and R. D. Rivarola, *Phys. Rev. Lett.* **87**, 023201 (2001).
- [9] A. L. Landers, E. Wells, T. Osipov, K. D. Carnes, A. S. Alnaser, J. A. Tanis, J. H. McGuire, I. Ben-Itzhak, and C. L. Cocke, *Phys. Rev. A* **70**, 042702 (2004).
- [10] M. E. Galassi, R. D. Rivarola, P. D. Fainstein, and N. Stolterfoht, *Phys. Rev. A* **66**, 052705 (2002).
- [11] N. Stolterfoht, B. Sulik, L. Gulyás, B. Skogvall, J. Y. Chesnel, F. Frémont, D. Hennecart, A. Cassimi, L. Adoui, S. Hossain, and J. A. Tanis, *Phys. Rev. A* **67**, 030702 (2003).
- [12] D. Misra, A. Kelkar, U. Kadhane, A. Kumar, L. C. Tribedi, and P. D. Fainstein, *Phys. Rev. A* **74**, 060701 (2006).
- [13] S. Chatterjee, D. Misra, A. H. Kelkar, L. C. Tribedi, C. R. Stia, O. A. Fojón, and R. D. Rivarola, *Phys. Rev. A* **78**, 052701 (2008).
- [14] J. S. Alexander, A. C. Laforge, A. Hasan, Z. S. Machavariani, M. F. Ciappina, R. D. Rivarola, D. H. Madison, and M. Schulz, *Phys. Rev. A* **78**, 060701 (2008).
- [15] K. N. Egodapitiya, S. Sharma, A. Hasan, A. C. Laforge, D. H. Madison, R. Moshhammer, and M. Schulz, *Phys. Rev. Lett.* **106**, 153202 (2011).
- [16] M. F. Ciappina, O. A. Fojón, and R. D. Rivarola, *J. Phys. B* **47**, 042001 (2014).
- [17] A. B. Voitkiv, B. Najjari, D. Fischer, A. N. Artemyev, and A. Surzhykov, *Phys. Rev. Lett.* **106**, 233202 (2011).
- [18] S. F. Zhang, D. Fischer, M. Schulz, A. B. Voitkiv, A. Senftleben, A. Dorn, J. Ullrich, X. Ma, and R. Moshhammer, *Phys. Rev. Lett.* **112**, 023201 (2014).
- [19] Although  $\lambda = 4$  a.u. substantially exceeds the “normal” size of  $H_2^+$  in the ground state, a noticeable fraction of  $H_2^+$  does have so large a size as the experiment shows [18].
- [20] N. Stolterfoht, R. D. DuBois, and R. D. Rivarola, *Electron Emission in Heavy Ion-Atom Collisions, Springer Series on Atomic, Optical, and Plasma Physics* (Springer, New York, 1997).
- [21] E. C. Montenegro, W. S. Melo, W. E. Meyerhof, and A. G. de Pinho, *Phys. Rev. Lett.* **69**, 3033 (1992).
- [22] W. Wu, K. L. Wong, R. Ali, C. Y. Chen, C. L. Cocke, V. Frohne, J. P. Giese, M. Raphaelian, B. Walch, R. Dörner, V. Mergel, H. Schmidt-Böcking, and W. E. Meyerhof, *Phys. Rev. Lett.* **72**, 3170 (1994).
- [23] R. Dörner, V. Mergel, R. Ali, U. Buck, C. L. Cocke, K. Froschauer, O. Jagutzki, S. Lencinas, W. E. Meyerhof, S. Nüttgens, R. E. Olson, H. Schmidt-Böcking, L. Spielberger, K. Tökesi, J. Ullrich, M. Unverzagt, and W. Wu, *Phys. Rev. Lett.* **72**, 3166 (1994).
- [24] J. H. McGuire, *Electron Correlation Dynamics in Atomic Collisions* (Cambridge University Press, Cambridge, England, 1997).
- [25] T. E. Sharp, *Atomic Data* **2**, 119 (1970).